Article

Dual-Mode Based Sliding Mode Control Approach for Nonlinear Chemical Processes

Camila Obando, Ruben Rojas, Francisco Ulloa, and Oscar Camacho*

Read Online

ACCESS | Metrics & More | Article Recommendations
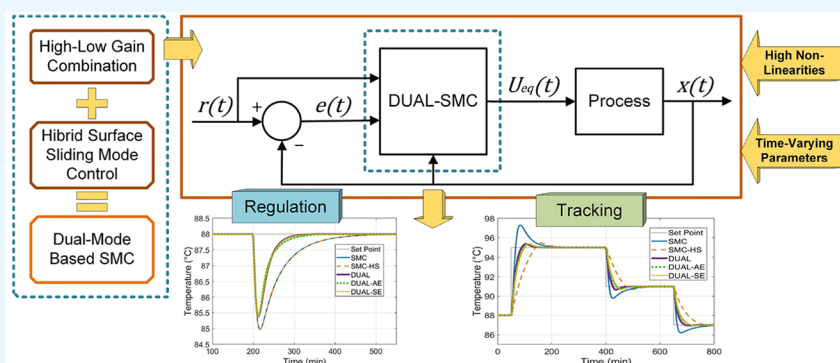
ABSTRACT: This paper synthesizes a new sliding mode controller (SMC) approach to enhance tracking and regulation tasks by following dual-mode concepts. The new control law consists of two distinct types of operation, using the combination of higher gain to large error signals (transient) and lower gain to small error signals (the region around the set point). The design is presented from a dual-mode (PD−PID) sliding surface operating in concert, fulfilling desired control objectives to ensure stability and performance. Therefore, a new controller was established, and we called it a dual-mode based SMC. The proposed controller is tested by computer simulations applied to two nonlinear processes, a continuous stirred-tank reactor (CSTR) and a mixing tank with a variable dead time. The results are compared with two different alternatives of SMC. In addition, the merits and drawbacks of the control schemes are analyzed using radial graphs, comparing the control methods with various performance measures for set points and disturbances changes. The ITSE (integral of time multiplied by the squared error), TVu (total variation of control effort) indices, Mp (maximum overshoot), and ts (settling time) were the indices used for performance analysis and comparisons.

1. INTRODUCTION

Chemical processes are complex, nonlinear, and higher-order. Moreover, chemical processes, especially at the industrial scale, are usually subjected to disturbances; these are mixed with the model uncertainties, nonmodeled dynamics, and nonwell-characterized plant parameters, decreasing conventional control performance.[1−3] Conveniently, robust controllers such as SMC are an alternative to solve the previously mentioned problems for chemical processes objectives and become a reason to use them for industrial processes; therefore, the robust controller allows for a rational resolution of conflicting control objectives.[4,5]

Sliding mode controller (SMC) is a nonlinear control technique based on variable structure controllers.[4−6] It gives the SMC some remarkable features as a robust control tool that responds suitably to nonlinear systems operating under uncertain conditions. Therefore, the SMC is useful because it is insensitive to the modeling deviation and the disturbances affecting those systems.[7−9]

The SMC brings the controlled variable from an initial condition to a desired final state, achieved through a sliding surface, representing the desired global behavior of the process output. Thus, a process behavior will depend on the surface parameters.[10,11] The sliding surface is used within the control law, which has two components, the continuous or sliding part and the discontinuous or reaching part.[5,10]

The complexity of the chemical processes, the lack of information on some process parameters, and process models relating to the controlled and manipulated variables are higher order. Hence, developing a complete model and controller is difficult for chemical processes.[1,12,13] As it is known, SMC is a
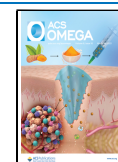
model-based control; thus, if phenomenological models are used, the resulting controller could be complex and could contain several adjustment parameters, resulting in challenging tuning work and troublesome implementation tasks, making the use of SMC unlikely in industrial applications.[13]

Empirical models are an alternative use for phenomenological models[4,12] for designing purposes. Empirical models use low-order linear models with dead time. Most of the time, first-order-plus dead time (FOPDT) models are empirical models suitable for chemical process control analysis and design[4,13] and recently[14] showed interesting results presenting a generalization of the FOPDT model for identification and control. It has been broadly used to capture the essential dynamic response of real-life processes for the control design system.[12,13]

In ref 4, a SMC was designed from a FOPDT to control nonlinear systems assuming that the controller robustness will compensate for the modeling errors resulting from linearizing the nonlinear process model. The SMC developed based on a FOPDT model of the actual process has been used for different approaches, as shown in refs 4, 10, 11, and 15−32.

Commonly used surfaces are PD-type and PID-type sliding surfaces.[5,33,34] PD surface reduces by one the order of the system, presenting a fast and smooth dynamic behavior. However, it can present a steady-state error and manage neither disturbances nor modeling errors. On the other hand, the PID surface allows the controller to carry out tracking and regulation. Conversely, overshoot and oscillations in the output are registered when a high controller gain is used due to the integral term in the PID surface.[4]

Considering that the chosen sliding surface type is associated with the SMC's overall operation, it is noticed that the selection or modification of the sliding surface can impact the performance of the SMC.[4] An option to improve SMC performance is presented in ref 32 in which the synthesis of a sliding mode controller considered a hybrid surface (SMC-HS) as an alternative to enhance the performance of the traditional SMC in its transient response. The control structure[32] switches between PD and PID sliding surfaces. The PD surface improves the tracking transient response against set point changes avoiding overshoot and oscillations, and switches to the PID surface when the system output is close to the desired set point to guarantee zero steady-state error. Even though ref 32 shows the potential of modifying an SMC switching between the two control laws, the resulting controller improves the transient response for tracking but not for the regulation task. Therefore, this improvement is not enough, which can be due to the initially designed controller gain (K_D) proposed by ref 4, which is conservative to avoid high overshoot and oscillations in the output caused by the PID sliding surface.

Feldbaum in 1960[35−38] introduced the dual control problem based on the idea that a controller operating on a system has two possibly conflicting goals; then, Shinskey[39] discussed the dual-mode (DM) control systems concepts. Dual-mode control is the combination or fusion of two controllers taking advantage of their features to produce a better performance than the single controllers; this combination operating sequentially in the same loop has been called a dual-mode system.[39−41] When two pre-established zones of operation exist in a particular application and the characteristics required for them cannot be achieved with a single controller, the dual control approach may be appropriate. For example, suppose a controller for each operation zone acts appropriately in its

respective zone. In that case, it may be essential to schedule these controllers so that each one operates in its zone and maximizes the benefits of its unique capabilities. The idea of using two different controllers between which the system switch depending on whether the system state is inside or outside some precalculated neighborhood of the operating point has been applied using different strategies.[42−48]

In this paper, the SMC proposed in ref 32 is modified to enhance both tracking and regulation tasks by following the DM concepts. The new control law consists of two distinct types of operation, using the combination of higher gain to large error signals (transient) and lower gain to small error signals (the region around the set point). The design is presented from a dual-mode sliding surface (PD−PID) operating in concert. Therefore, a new controller was established, and we called it a dual-mode based sliding mode controller.

The proposed controller is tested by computer simulations, comparing its results with a traditional SMC[4] and the SMC-HS.[32] In addition, The merits and drawbacks of the control schemes are analyzed using radial graphs, comparing the control methods with different performance measures for set points and disturbances changes. The ITSE, TVu, Mp (maximum overshoot), and ts (settling time)[49] were the performance indices used for analysis and comparisons.

The contributions of this study can be summarized as follows:

- Following the dual-mode concepts, a new dual-mode sliding mode controller is established. The new controller uses higher gain to large error signals (transient) and lower gain to small error signals (the region around the set point) to enhance tracking and regulation tasks.

- The dual-mode sliding mode control structure changes between PD and PID sliding surfaces. The PD surface improves the tracking transient response against set point changes avoiding overshoot and oscillations, and switches to the PID surface when the system output is close to the desired set point to guarantee zero steady-state error.

In summary, a dual-mode system combines two controllers that operate consecutively in the same loop and combine or fuse their best characteristics to create a superior performance to the single controllers. To our knowledge, no dual-mode sliding mode controller (DM-SMC) has been presented in other works.

The rest of the paper is organized as follows: section 2 presents the sliding mode control and dual mode systems fundamental concepts. Section 3 shows how the new dual-mode sliding mode controller is synthesized. The nonlinear systems for controller tests, their results, and discussions are described in section 4. Finally, conclusions are summarized in section 5.

2. BACKGROUND

This section presents a brief description of SMC and the concept of dual-mode systems.

2.1. Sliding Mode Control Fundamentals. The SMC is a variable structure controller developed using nonlinear control techniques.[5,6] It is also a robust control that responds adequately to nonlinear systems operating under uncertain conditions.[5,6,50] Furthermore, it is insensitive to the variation

of modeling parameters once it finds the sliding mode of its scheme.[8] The SMC considers a sliding surface that allows the controlled variable to pass from an initial state to a desired final state. For this, its control law comprises a continuous part, which has to do with the sliding part, and a discontinuous part for the reachability phase. The corresponding sliding surface scheme is presented in Figure 1.
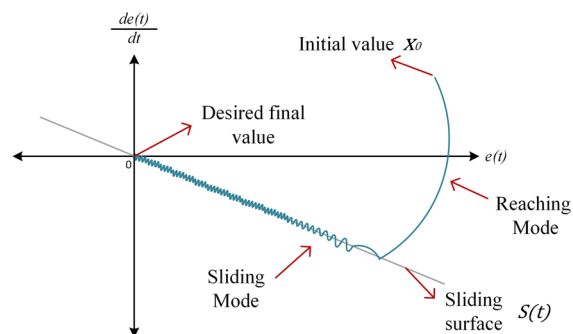
Figure 1. Schematic of the SMC sliding surface.

For the sliding part, it is sought that there is no variation in the surface, and for the reachability phase, it is required to reach the sliding surface, which is $S(t)$ equal to zero. So then, the design stages for an SMC are first, define the surface, and second, synthesize the control law based on that surface.[5,6]

Therefore, it is essential to select a sliding surface according to the response expectations of the process. The sliding surface is where the system dynamics are restricted to its equations.[10,19] Then, the behavior of a process will depend on the surface dynamics. Moreover, the chosen surface will represent the desired global performance and characterize the stability of the whole system.[5,31]

The usual choice is the PID surface.[5] However, a more highly sensitive controller could be achieved if a proportional-derivative action is considered. Indeed, PD responds to the rate of change of the error, which is corrected with anticipation. The control action becomes opportune without allowing the magnitude of the error to become too large.[8,12] However, the weaknesses of a derivative action, such as its susceptibility to noise, are well-known, but PD benefits cannot be ignored either.

2.2. Dual-Mode Systems Concepts. Feldbaum introduced the idea of dual control,[35−38] and then Shinskey[39] discussed the DM Control systems concepts. Different strategies have been applied using two distinct controllers between which the system switches depending on whether the system state is within or outside a predetermined operating point neighborhood.[42−48] Ref 39 considers the best controller under the analysis of the process response characteristics such as maximum speed, critical damping, no offset, and noise sensitivity.

Thus, any control system that can satisfy the above requirements also meets any minimum performance indices, no matter what function of the error may be used and, in any case, the nature of the input signals.

The nature of the process defines the controller design, which produces the best loop performance, and characterizes the controller's difficulty in accomplishing the objectives listed above. As the process complexity increases, single controllers cannot get the best or optimum performance. However, a combination of them should increase performance and stabilize the process. As a result, combining or merging two controllers to use their individual capabilities results in performance superior to that of the single controller; this combination, which operates consecutively in the same loop, is known as a dual-mode system.[39] The corresponding scheme of operation and the logic for the sequence of action of each controller will be shown later in Figures 2 and 3.

3. DUAL-MODE SLIDING MODE CONTROLLER SYNTHESIS

This section 3 describes the methodology to synthesize the dual-mode sliding mode controller (DUAL-SMC). The DUAL-SMC proposal enhances tracking and regulation based on the dual-mode control concepts.[39] The combination sought of both higher gain to large error signals and lower gain to small error signals, as control actions appropriated to produce the desired output, has not a unique solution. Consequently, after the first requirements are fulfilled, additional objectives concerning the traditional SMC design are required to obtain a well-defined control problem.

The desired control objectives that must be accomplished are, therefore, as follows: (1) To obtain a stable PD sliding mode control law for the "transient region" of the system response. (2) To obtain a stable PID Sliding Mode Control law for the "around the steady-state region". (3) To obtain an appropriate (high gain)/(low gain) relationship for the PD/PID control laws to ensure a smooth response. (4) To obtain smooth switching between control laws to ensure nominal closed-loop stability.

The original sliding mode control law[4] was oriented to high-order nonlinear chemical processes represented by reduced-
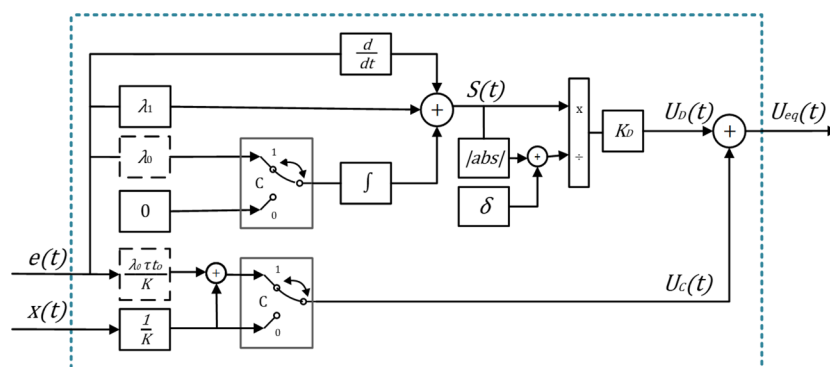
Figure 2. Block diagram scheme of the dual-mode sliding mode controller (DUAL-SMC).
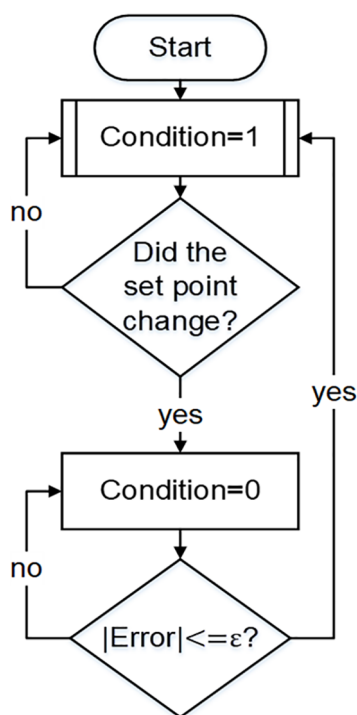
Figure 3. Condition C operating logic flowchart.

order system models such as FOPDT models; therefore, working with a FOPDT model as the one presented in eq 1 is convenient as a base for the following development:

$$G_p(s) = \frac{K}{\tau s + 1} e^{-t_0 s} \tag{1}$$

Here, K is the gain, τ is the time constant, and t_0 is the dead time.[13] These three parameters are the minimum number of identifiers that a FOPDT model requires.

In ref 4, it is explained why using the Pade approximation for the SMC controller design is not recommended. Therefore, a first-order Taylor series approximation is suggested to convert better the dead time term that appears in eq 1. The Pade approximation introduces a right-half plane zero that produces an inverse response term in the resulting model. When the equivalent procedure controller design is applied, it creates an unstable controller; therefore, the Pade approximation can not be used directly to replace the dead time term. Thus, in ref 4 is proposed a first-order Taylor series expansion, adding one more pole that can be included to $G_p(s)$ with the value of the time delay and then getting the expression that eq 2 holds:

$$G_p(s) = \frac{x(s)}{U(s)} \cong \frac{K}{(\tau s + 1)(1 + t_0 s)} \tag{2}$$

Eq 2 is represented in the time domain in eq 3. It characterizes the previous relationship of the transfer function $G_p(s)$ by stating the system output $x(t)$ to its input $U(t)$ as a function of time. This frequency–time domain conversion can be found with the inverse Laplace transformation:

$$\frac{d^2 x(t)}{dt^2} + \frac{(\tau + t_0)}{(\tau t_0)} \frac{dx(t)}{dt} + \frac{1}{(\tau t_0)} x(t) = K \frac{U(t)}{(\tau t_0)} \tag{3}$$

3.1. PD-SMC Design. The first step in designing an SMC is to propose a sliding surface $S(t)$. Generally, the surface could be defined as expressed in eq 4:[34]

$$S(t) = \left(\frac{d}{dt} + \lambda\right)^{n-1} e(t) \tag{4}$$

Then, the complexity of the surfaces is related to the order of the system n. There, λ is a tuning parameter chosen according to the desired system dynamics, and $e(t)$ is the error between the set point and the process output. The process model (eq 3) represents a second-order system. So, for n equal to two, eq 4 can be expanded as follows:

$$S_1(t) = \frac{de(t)}{dt} + \lambda e(t) \tag{5}$$

this structure has the form of a PD-type controller. Then, it is possible to develop an SMC control law $U(t)$, as expressed in eq 6:

$$U(t) = U_C(t) + U_D(t) \tag{6}$$

where $U_C(t)$ is the continuous component of the control law that ensures the sliding mode, and $U_D(t)$ is the discontinuous part, also known as reachability control law,[40,51] responsible for the reaching mode. It is well-known from the sliding mode literature that choosing the control law is established by eq 6,[51] allowing easy verification of the sliding mode sufficiency conditions and reachability. That means the $S(t) = 0$ condition is satisfied first when the system reaches the sliding mode, that is, when $U_D(t) = 0$, (equivalently $S(t) = 0$) and then by the equivalent control principle $U_{eq} = U_C(t)$ will maintain the system on the sliding surface (again $S(t) = 0$).

The continuous control law $U_C(t)$ is determined using Filippov's equivalent control procedure[31,40] following the sliding mode desired motion. The first step is to apply the sliding condition (eq 7):[31]

$$\frac{dS(t)}{dt} = 0 \tag{7}$$

Thus, the chosen surface is derived:

$$\frac{dS_1(t)}{dt} = \frac{d^2 e(t)}{dt^2}(t) + \lambda \frac{de(t)}{dt} = 0 \tag{8}$$

Afterward, the output error $e(t)$ is expressed in terms of the system output $x(t)$ and the set point $r(t)$. Considering that $e(t) = r(t) - x(t)$, eq 8 is rewritten as follows:

$$\frac{d^2 r(t)}{dt^2} - \frac{d^2 x(t)}{dt^2} + \lambda \frac{dr(t)}{dt} - \lambda \frac{dx(t)}{dt} = 0 \tag{9}$$

Since most chemical process control operates in regulation, a set point or reference can typically be considered constant;[13] thus, the derivatives of the reference are zero. However, when a set point or reference change occurs,[4] it has been shown that the derivatives of the reference value can be omitted without degrading the controller's performance, making the process simpler and preventing the kicking effect on the final control element. Thus, the previous equation can be written as follows:

$$-\frac{d^2 x(t)}{dt^2} - \lambda \frac{dx(t)}{dt} = 0 \tag{10}$$

Substituting eq 10 in eq 3 and rearranging, $U_C(t)$ is obtained as expressed in eq 11:

$$U_C(t) = \frac{\tau t_0}{K} \left[\frac{x(t)}{\tau t_0} + \left(\frac{\tau + t_0}{\tau t_0} - \lambda \right) \frac{dx(t)}{dt} \right] \tag{11}$$

On the other hand, the reachability control law $U_D(t)$ is nonlinear and is mainly designed based on the sign function with a hypothetical infinitely fast speed. However, to reduce chattering, the relay-like function is replaced by a sigma function of the surface and constant parameters, which can be written as follows:

$$U_D(t) = K_D \frac{S(t)}{|S(t)| + \delta} \tag{12}$$

where K_D is the tuning gain, which is responsible for the reaching mode, and δ for reducing the chattering effect. So, the SMC control law $U_1(t)$ (eq 6) for the proposed PD sliding surface[34] can be written as

$$U_1(t) = \frac{\tau t_0}{K}\left[\left(\frac{\tau + t_0}{\tau t_0} - \lambda\right)\frac{dx(t)}{dt} + \frac{x(t)}{\tau t_0}\right] + K_{D1}\frac{S_1(t)}{|S_1(t)| + \delta_1} \tag{13}$$

In general, the stability of the SMC systems is obtained if two conditions are fulfilled: (a) the sliding surface is stable, which depends on the choice of λ, and (b) the sliding surface is reached in a finite time that can be ensured if the reachability condition is satisfied. This condition comes from Lyapunov's stability criteria as follows: First, consider the following Lyapunov candidate function:

$$V(t) = \frac{1}{2}S^2(t) \tag{14}$$

Then, taking the derivative of the candidate function of Lyapunov, we obtain

$$\frac{dV(t)}{dt} = S(t)\frac{dS(t)}{dt} \tag{15}$$

From Lyapunov's stability theorem, any linear or nonlinear system is globally asymptotic stable if $dV(t)/dt$ is negative definite; then, for reaching the sliding surface in a finite time, the following condition must be satisfied:

$$S(t)\frac{dS(t)}{dt} < 0 \tag{16}$$

which is known as the reachability condition in the sliding mode literature.[44] A stronger condition, ensuring an ideal sliding motion, is the η-reachability condition given by

$$S(t)\frac{dS(t)}{dt} \leq -\eta|S| \tag{17}$$

where η is a small positive constant.[50]

Assuming that the change in set point and the system disturbances can be represented by an external disturbance $d(t)$ that enters the system through the input channel (matched uncertainty). It holds that the disturbance $d(t)$ is bounded with a known upper bound, which means there exists d_0 such that $\sup_t \geq 0|d(t)| \leq d_0$. Therefore, the system time (eq 3) can be rewritten as

$$\frac{d^2x(t)}{dt^2} + \frac{\tau + t_0}{\tau t_0}\frac{dx(t)}{dt} + \frac{1}{\tau t_0}x(t) = K\frac{U(t) + d(t)}{\tau t_0} \tag{18}$$

Writing the derivative of the candidate function of Lyapunov (eq 15) for the proposed PD sliding surface,

$$\frac{dV_1(t)}{dt} = S_1(t)\frac{dS_1(t)}{dt}$$
$$= S_1(t)\left(\frac{d^2r(t)}{dt^2} - \frac{d^2x(t)}{dt^2} + \lambda\frac{dr(t)}{dt} - \lambda\frac{dx(t)}{dt}\right) \tag{19}$$

solving $d^2x(t)/dt^2$ from eq 18, replacing in eq 19, and discarding the derivatives of the reference:

$$\frac{dV_1(t)}{dt} = S_1(t)\left(\frac{t_0 + \tau}{t_0\tau}\frac{dx(t)}{dt} + \frac{x(t)}{t_0\tau} - \frac{K(U(t) + d(t))}{t_0\tau} - \lambda\frac{dx(t)}{dt}\right) \tag{20}$$

The control law of eq 13 is replaced in the previous eq:

$$\frac{dV_1(t)}{dt} = S_1(t)\left\{\frac{t_0 + \tau}{t_0\tau}\frac{dx(t)}{dt} + \frac{x(t)}{t_0\tau} - \frac{K}{t_0\tau}\left[\frac{\tau t_0}{K}\left[\frac{x(t)}{\tau t_0} + \left(\frac{\tau + t_0}{\tau t_0} - \lambda\right)\frac{dx(t)}{dt}\right] + K_{D1}\frac{S_1(t)}{|S_1(t)| + \delta_1} + d(t)\right] - \lambda\frac{dx(t)}{dt}\right\} \tag{21}$$

Simplifying:

$$\frac{dV_1(t)}{dt} = S_1(t)\left(-\frac{K}{t_0\tau}\left[K_{D1}\frac{S_1(t)}{|S_1(t)| + \delta_1} + d(t)\right]\right)$$
$$= -\frac{KK_{D1}}{t_0\tau}\frac{|S_1(t)|^2}{|S_1(t)| + \delta_1} - \frac{K}{t_0\tau}d(t)S_1(t) \tag{22}$$

Now for $\delta > 0$, α is defined as

$$\alpha = \frac{|S_1(t)|}{|S_1(t)| + \delta_1} \quad \text{then } 0 < \alpha < 1 \tag{23}$$

So eq 22 can be written as

$$\frac{dV_1(t)}{dt} = -\frac{KK_{D1}\alpha}{t_0\tau}|S_1(t)| - \frac{K}{t_0\tau}d(t)S_1(t)$$
$$\leq -\frac{KK_{D1}\alpha}{t_0\tau}|S_1(t)| + \left|\frac{K}{t_0\tau}d(t)\right||S_1(t)| \tag{24}$$

Then

$$\frac{dV_1(t)}{dt} \leq -\left(\frac{KK_{D1}\alpha}{t_0\tau} - \left|\frac{K}{t_0\tau}d(t)\right|\right)|S_1(t)| = -\eta|S_1(t)| \tag{25}$$

Therefore, to fulfill eq 25, it is a necessary condition that

$$\eta = \left(\frac{KK_{D1}\alpha}{t_0\tau} - \left| \frac{K}{t_0\tau} d(t) \right| \right) > 0 \tag{26}$$

because t_0 and τ are always positive, and d_0 bounds $d(t)$, this condition can be simplified as

$$((KK_{D1}\alpha - |K||\delta(t)|) > 0) \quad or \quad (KK_{D1}\alpha > |K|d_0) \tag{27}$$

that is

$$\begin{cases} K_{D1} > d_0/\alpha & \text{if} \quad K > 0 \\ K_{D1} < -d_0/\alpha & \text{if} \quad K < 0 \end{cases} \tag{28}$$

Considering the previous eq, for the sliding surface to be reached in a finite time, K_{D1} must be defined as

$$K_{D1} = \text{sign}(K)\beta_1 d_0 \quad \text{for any } \beta_1 > 1 \tag{29}$$

3.2. PID-SMC Design. Similar to the PD-type situation, identifying the sliding surface $S(t)$ is the initial step in building an SMC. For example, to get an integral control, the surface could be specified as shown in eq 30:[34]

$$S(t) = \left(\frac{d}{dt} + \lambda \right)^n \int e(t) \, d(t) \tag{30}$$

Again, process model (eq 3) represents a second-order system. So that eq 30 can be expanded for n equal to two as follows:

$$S_2(t) = \frac{de(t)}{dt} + \lambda_1 e(t) + \lambda_0 \int e(t) \, d(t) \tag{31}$$

This controller design is the traditional SMC developed by ref 4. Then, following the procedure shown in the previous section, the PID SMC controller can be summarized as follows: the SMC control law $U(t)$ (eq 6) for the proposed PID sliding surface can be written as

$$U_2(t) = \frac{\tau t_0}{K} \left[\left(\frac{\tau + t_0}{\tau \, t_0} - \lambda_1 \right) \frac{dx(t)}{dt} + \frac{x(t)}{\tau \, t_0} + \lambda_0 e(t) \right]$$
$$+ K_{D2} \frac{S_2(t)}{|S_2(t)| + \delta_2} \tag{32}$$

Again, the stability of the system when the PID SMC control law is applied is obtained if the following conditions are fulfilled: (a) the sliding surface is stable, which depends on the choice of the parameters (λ_1 and λ_0), and (b) the sliding surface is reached in a finite time that can be ensured as in the previous case satisfying the η-reachability condition. So, K_{D2} must be defined as

$$K_{D2} = \text{sign}(K)\beta_2 d_0 \quad \text{for any } \beta_2 > 1 \tag{33}$$

Camacho and Smith[4] give expressions to calculate the traditional SMC control law setting values. In this case, λ_1 is chosen to obtain a simple controller structure, λ_0 to guarantee the PID sliding surface stability, the parameter K_D related to the speed to reach the surface was optimally determined to guarantee low overshoot,[4] and similarly δ to soften the system response avoiding chattering problems:

$$\lambda_1 = \frac{\tau + t_0}{\tau t_0} \tag{34}$$

$$\lambda_0 \le \frac{\lambda_1^2}{4} \tag{35}$$

$$K_D = \frac{0.51}{|K|} \left(\frac{\tau}{t_0} \right)^{0.76} \tag{36}$$

$$\delta = 0.68 + 0.12|K|K_D\lambda_1 \tag{37}$$

Hereafter, the original value proposed for the parameter K_D (eq 36) will be named K_{DO}.

3.3. Determination of (High Gain)/(Low Gain) Relationship for PD/PID Control Laws. The proposed control law shown in ref 32 offers improvements in tracking by avoiding overshoot and oscillations, but does not affect regulation. This can be due to the conservative value given by K_{DO} defined for a PID SMC control law acting alone, but the previous η-reachability condition calculations set no upper bound for $|K_{D1}|$ and $|K_{D2}|$. Theoretically, the most demanding reference change is the step input. This is from the approach that implies that the reference tracking of a step signal demands an instantaneous change from a stationary state to a new one without going through a transitory phase. This could be understood as the need for a controller with infinite gain.[36] However, the speed at which a variable may change is limited; for this reason, less conservative values based on the traditional control law can be adopted, namely: $|K_{D1}| = H \times K_{DO}$ and $|K_{D2}| = L \times K_{DO}$ for any H and L positive scalars. This gives a H/L relationship for (High Gain)/(Low Gain) for the designed PD and PID SMC controllers, respectively. However, switching from a high constant gain to a lower one can disturb the system performance despite both gains fulfilling the reachability condition.

The transition between the gains of the two reaching control laws can be softened if the nonlinear gains can be proposed as follows:

$$K_{D1} = K_{D2} = K_{DO}(\rho + \gamma|e(t)|) \text{ or } K_{D1} = K_{D2} = K_{DO}$$
$$(\theta + \varphi e(t)^2) \tag{38}$$

note that ρ, γ, θ, and ϕ can be calculated to obtain the previously proposed H/L relationship as follows:

$$\rho + \gamma e_{\max} = H; \quad \rho + \gamma e_{\min} = L;$$
$$\theta + \varphi e_{\max}^2 = H; \quad \theta + \varphi e_{\min}^2 = L \tag{39}$$

Therefore:

$$\gamma = \frac{H - L}{e_{\max} - e_{\min}}; \quad \rho = L - \gamma e_{\min};$$

$$\varphi = \frac{H - L}{e_{\max}^2 - e_{\min}^2}; \quad \theta = L - \varphi e_{\min}^2 \tag{40}$$

where $e_{\max}$ is an estimated positive upper bound for the system output error, and $e_{\min}$ is a positive constant that defines the error limit where the output enters the "around steady-state region" of the system response. The proposed three approaches will be tested in the computer simulation section.

3.4. Smooth Switching. By definition, the proposed dual-mode sliding mode controller system has just two possibilities of switching: (a) from the "around steady-state region" to the "transient region" by a step set point change at any time t_{c1} and (b) from the "transient region" to the "around steady-state region" when the output error reaches the band of small errors

(e_{min} limited) at any time t_{c2}. So, to obtain smooth switching, we must establish not growing conditions like those defined by Beker et al.,[52] so

$$\begin{cases} \triangle V_1(t_{c1}) = V_2(t_{c1}) - V_1(t_{c1}) \leq 0 \text{ at any time } t_{c1} \\ \triangle V_2(t_{c2}) = V_2(t_{c2}) - V_2(t_{c2}) \leq 0 \text{ at any time } t_{c2} \end{cases} \quad (41)$$

Then

$$\triangle V_1(t_{c1}) = V_2(t_{c1}) - V_1(t_{c1}) = \frac{1}{2}S_2{}^2(t_{c1}) - \frac{1}{2}S_1{}^2(t_{c1}) \leq 0$$

at any time t_{c1} (42)

$$\triangle V_2(t_{c2}) = V_1(t_{c2}) - V_2(t_{c2}) = \frac{1}{2}S_1{}^2(t_{c2}) - \frac{1}{2}S_2{}^2(t_{c2})$$

$$\leq 0 \text{ at any time } t_{c2} \quad (43)$$

Therefore

$$\left(\frac{de(t_{c1})}{dt} + \lambda_1 e(t_{c1}) + \lambda_0 \int e(t_{c1}) \, dt \right)^2$$
$$- \left(\frac{de(t_{c1})}{dt} + \lambda e(t_{c1}) \right)^2 \leq 0 \text{ at any time } t_{c1} \quad (44)$$

$$\left(\frac{de(t_{c2})}{dt} + \lambda e(t_{c2}) \right)^2$$
$$- \left(\frac{de(t_{c2})}{dt} + \lambda_1 e(t_{c2}) + \lambda_0 \int e(t_{c2}) \, dt \right)^2$$
$$\leq 0 \text{ at any time } t_{c2} \quad (45)$$

Looking at eqs 44 and 45, it is evident that there is not a trivial solution due to the integral term. Now, if $S_1(t)$ is redefined as follows:

$$S_1{}^*(t) = S_1(t) + C^* = \frac{de(t)}{dt} + \lambda e(t) + C^* \quad (46)$$

Then, $\dot{S}_1{}^*(t) = \dot{S}_1(t)$. Consequently, all section 3.1 holds. Now replacing $S_1(t)$ in eqs 44 and 45 by $S_1{}^*(t)$ the following conditions are obtained:

$$\left(\frac{de(t_{c1})}{dt} + \lambda_1 e(t_{c1}) + \lambda_0 \int e(t_{c1}) \, dt \right)^2$$
$$- \left(\frac{de(t_{c1})}{dt} + \lambda e(t_{c1}) + C^* \right)^2 \leq 0 \text{ at } t_{c1} \quad (47)$$

$$\left(\frac{de(t_{c2})}{dt} + \lambda e(t_{c2}) + C^* \right)^2$$
$$- \left(\frac{de(t_{c2})}{dt} + \lambda_1 e(t_{c2}) + \lambda_0 \int e(t_{c2}) \, dt \right)^2 \leq 0 \text{ at } t_{c2} \quad (48)$$

This is fulfilled only for equality if and only if:

$$\begin{cases} \lambda = \lambda_1 \\ C^* = \lambda_0 \int e(t_{c1}) \, dt = \lambda_0 \int e(t_{c2}) \, dt \end{cases} \quad (49)$$

The previous equation indicates that smooth switching can be achieved when $\lambda = \lambda_1$ and the integral term remains constant throughout the "transient region". As a result, for the controller approach to work properly, λ needs to be adjusted to λ_1. Furthermore, the integral term needs to be kept at the same value throughout the "transient region" which is obtained by making the input to the integral equal to zero, as shown in Figure 2.

3.5. Dual-Mode Sliding Mode Controller Implementation. The block representation of the proposed controller (DUAL-SMC) is shown in Figure 2. There, the parameters λ_0, λ_1, and δ are obtained with the eqs 34, 35, and 37, respectively. The K_D block represents the nonlinear gain described in section 3. Either the change between fixed gains (H/L) or one of the expressions in eq 38 can be used to obtain K_D.

As mentioned in section 3.4, the dual-mode sliding mode controller has two switching possibilities: (a) from the "around steady-state region" to the "transient region" that is identified with condition C equal to 0 when a set point change occurs; and (b) from the "transient region" to the "around steady-state" identified with condition C equal to 1, when the error becomes less than an ε value (e_{min}), which is defined as considering the process response. It can be defined at a certain percentage, such as 2% or 5% of the output error $e(t)$ concerning the actual set point. The operating logic is shown in Figure 3.

Finally, the DUAL-SMC depends on the error, the system output, and the given set point. Its scheme is shown in Figure 4.
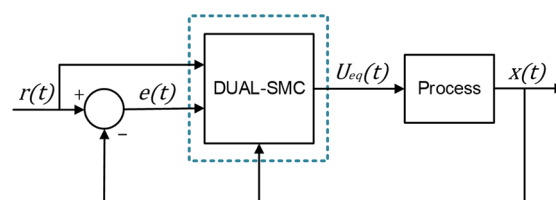
Figure 4. DUAL-SMC within the control loop.

4. RESULTS AND DISCUSSIONS

This section presents two nonlinear chemical process examples chosen to test the performance of the dual-mode SMC approaches. First, a CSTR is presented to perform regulatory and tracking tests. Second, a mixing tank with variable dead time is used. It is focused on the regulatory tasks when the dead time varies to see how the controllers work when a variation in process parameters occurs. A detailed description of each process, with mathematical modeling and their parameter values, is given in ref 10. It is essential to mention that methodologically, two parts are presented. First, the reaction curve procedure is applied from the nonlinear process, and the characteristics parameters (K, τ, and t_0) are obtained and used in the controller equations. Second, the controllers are applied to the nonlinear processes.

Five control schemes (SMC, SMC-HS, and three different DUAL-SMC possibilities) are tested and compared. The three DUAL scheme variations considered are based on the different K_D used. First, K_D is switched between ($K_D = H \times K_{DO}$) and ($K_D = L \times K_{DO}$) with a constant ratio (DUAL-SMC) for the "transient region" and the "around the steady-state region", respectively. Then, two nonlinear gains, one based on the

absolute error ($K_D = K_{DO}(\rho + \gamma|e(t)|)$) and others based on the square error ($K_D = K_{DO}(\theta + \phi e(t)^2)$), denoted as DUAL-AE and DUAL-SE, respectively.

In both examples, process output, control action, and K_D evolution for all the controllers are compared and contrasted. Furthermore, radial graphs presenting performance indices and transient criteria such as maximum overshoots and settling times are used as performance measures for the different controllers.

4.1. Chemical Reactor. This first example concerns a chemical reactor. It plays an essential role in industrial chemical processes and is the container where the chemical reaction occurs.[53,54] The reactor shown in Figure 5 is a
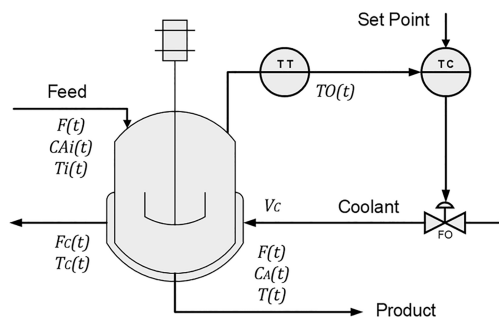
Figure 5. Continuous stirred tank reactor process diagram.

continuous-stirred tank where $A \rightarrow B$ exothermic reaction occurs. Many processes are exothermic. One can particularly refer to the radical polymerization of acrylates, such as in ref 55. The surrounding jacket eliminates the heat of the reaction through which a cooling liquid flow. The equations of the nonlinear model and operating conditions of this process are presented in ref 4.

During this process, the transmitter manages a range from 80 to 100 °C, and the valve handles values from 0 to 1. The output temperature of the product is 88 °C. For this reactor, regulation and tracking tests are carried out.

From the reaction curve procedure described by,[13] a FOPDT model approximation is obtained. The FOPDT model, with its characteristic parameters, is shown as follows:

$$G_{p2}(s) = \frac{1.66}{12.75s + 1} e^{-7.11s} \tag{50}$$

Once the values presented in eq 1 for the reduced-order system model K, τ, and t_0 are known by using the reaction curve procedure,[16] the values of λ_0, λ_1, δ, and K_{DO} can be calculated using eqs 34–37. Meanwhile, the values of the design parameters for the dual schemes H, L, e_{max}, and e_{min} were chosen considering the a priori knowledge of the process: First, H and L give the relationship for (High Gain)/(Low Gain) of the dual-mode concerning the original K_{DO} such that a 3/2 ratio can be considered to make the controllers more aggressive. Second, e_{max} is an estimated positive upper bound for the system output error, because a transmitter with a 0 to 1 span is used to measure the process output, $e_{max} = 0.5$ is the right choice for this parameter. Finally, e_{min} is a positive constant that defines the error limit where the output enters the "around steady-state region" of the system response and, as it was pointed out previously, can be defined at a certain percentage, such as 2% or 5% of the output error $e(t)$ in respect to the current set point. Therefore, because the

maximum set point change to be considered is about 10 °C, which is equivalent to 0.5 transmitter fraction of the output, then $e_{min} = 0.05 \times (0.5) = 0.025$ can be considered for 5% of the output error choice. Table 1 details the controllers' remaining parameter values for this process.

Table 1. Controllers Parameter Values

parameter	controller				
	SMC	SMC-HS	DUAL	DUAL-AE	DUAL-SE
K_{D0}	0.6519				
λ_0	0.0209				
λ_1	0.2890				
δ	0.7175				
γ				2.1053	
ρ				1.9474	
ϕ					4.0100
θ					1.9975
$K_D|_{e(t)=0}$	K_{D0}	K_{D0}	1.3038	1.2695	1.3022

4.1.1. Regulation Performance Test. Disturbances at the feed flow temperature are simulated to test the performance of controllers in the regulation task. Two changes of −10% in the inlet temperature are introduced at 200 and 800 min. The simulated variations in the temperature T_i are shown in Figure 6.
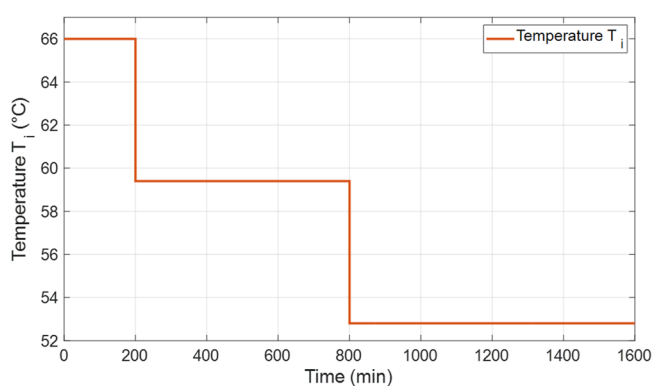
Figure 6. Simulated variations in the feed flow temperature, T_i.

Figure 7 shows how all the SMC approaches compensate for the disturbances. The process responses for the SMC and SMC-HS controllers are equal; they are overlapped since they
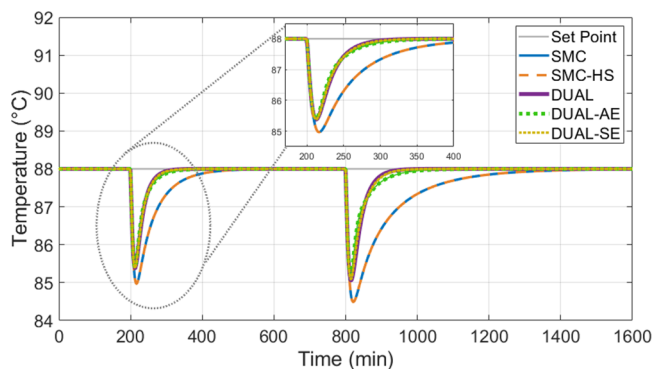
Figure 7. System outputs for the different controllers when T_i disturbances are simulated.

have the same gain, K_{DO}. In the same way, the outputs of the DUAL-mode SMC schemes are close to each other. An improvement in regulation occurs due to the proposed change in the reaching mode gain, K_D. The proposed DUAL-mode SMC controllers are faster than the SMC and SMC-HS schemes to reject the inlet temperature disturbances. In the beginning, the system output response for the DUAL-AE controller against the second disturbance, the coldest inlet temperature, is sharper than those for the DUAL and DUAL-SE controllers but presents a longer settling time.

Figure 8 shows all the SMC controllers' outputs, and their responses are by the observed temperature response. The
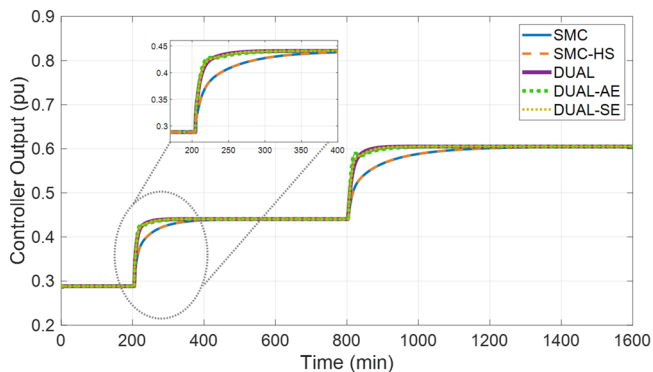
Figure 8. Control outputs for the different controllers when T_i disturbances are simulated.

Dual-Mode controllers act faster without abrupt changes that can deteriorate the final control element.

Figure 9 shows K_D evolution for the different controllers. The SMC and SMC-HS controller gains are smaller than those
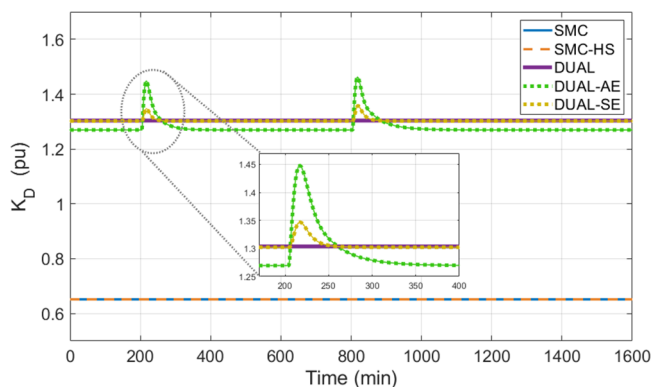
Figure 9. Evolution over time of K_D for the regulation performance test.

for the dual-mode SMC, giving a sluggish performance. Furthermore, there is no switching between the "around steady-state region" and the "transient region" because no set point change occurs during this test since only regulation tasks are performed. So, when the disturbances occur, the system remains on the "the steady-state region," and when the output error $e(t)$ increases in magnitude, the nonlinear gain functions (DUAL-AE and DUAL-SE) act, increasing smoothly to correct the error.

The DUAL-AE gain presents a higher peak value than the DUAL-SE, requiring a minor variation to compensate for the error. At steady-state, the DUAL and DUAL-SE gains are close

to each other and slightly higher than the DUAL-AE gain, giving the desired aggressiveness established by the design parameter L for the "around the steady-state region".

Remarkably, the DUAL schemes can compensate for disturbances at around 40% of the time taken for the SMC and SMC-HS schemes, which can be seen in the radial graph in Figure 10.
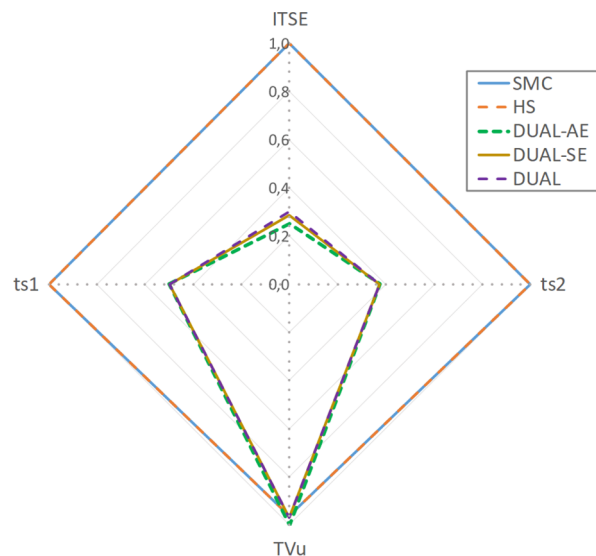
Figure 10. Radial graph for regulation.

When comparing performance indices and transient criteria in each radial graph vertices, all the values for each criterion are observed simultaneously. Hence, the best result is that one with the polygon with the smallest area because it indicates that, in general terms, it corresponds to the scheme that best balances all its indicators with minimum values.

This radial graph compares ITSE and TVu indices. Furthermore, as criteria of the transient response, the times, t_{s_1} and t_{s_2} in which the disturbances are compensated, and the reference is reached. As SMC and SMC-HS are of fixed structure, they do not indicate improvement in the speed of compensation (t_s), unlike the dual schemes that reduce their value up to 40% of the original. As for ITSE, the integral of the quadratic error can be reduced to 30%. All these improvements while maintaining a similar value in TVu. In other words, with the same control effort, it is possible to have a faster transition time and compensate for disturbances.

4.1.2. Tracking Performance Test. For the tracking test, four reference changes are simulated at times 50, 400, 650, and 870 min; the temperature set point of the chemical reactor is varied from the original 88 °C to 95, 91, 87, and 97 °C, respectively.

Figure 11 shows the process output for the tracking performance test. The proposed dual-mode SMC controllers perform better than the traditional SMC and SMC-HS controllers. This can be noticed at first sight, observing that the process outputs for the proposed dual-mode SMC give smaller overshoots than the corresponding output for the standard SMC controller. Moreover, the dual-mode SMC reach the steady-state faster than the process output responses for both the traditional SMC and the SMC-HS controllers.

Regarding the controller outputs, Figure 12 depicts when set point changes are introduced in the simulation. Again, the
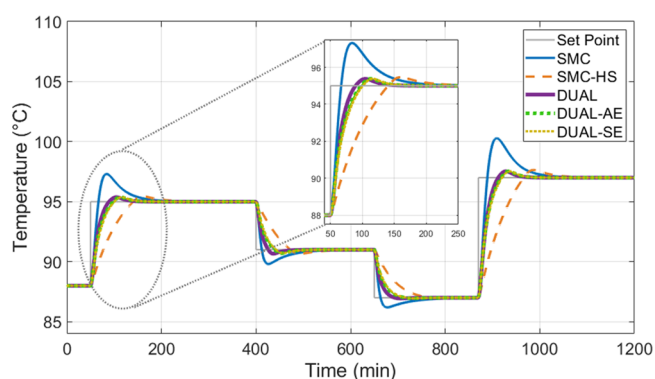
Figure 11. System output responses for the different controllers when simulated set point changes are introduced.
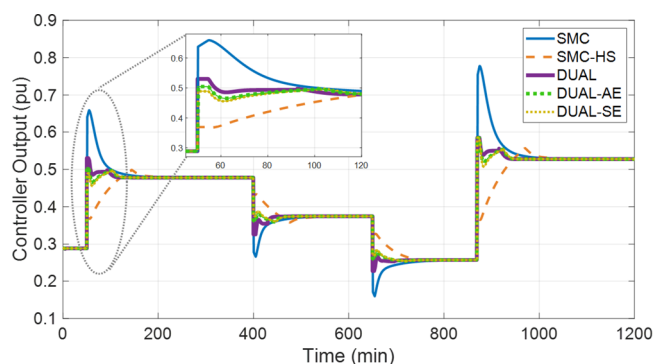
Figure 12. Control output for set point changes.

smoothest control actions come from the SMC-HS, while the traditional SMC presents an abrupt change under the observed temperature response. On the other hand, dual-mode controller schemes initially have fast action but are not as abrupt as the traditional SMC controller; therefore, their temperature responses present smaller overshoots.

Figure 13 shows K_D evolution for the different controllers. The SMC and SMC-HS controller gains are smaller than the
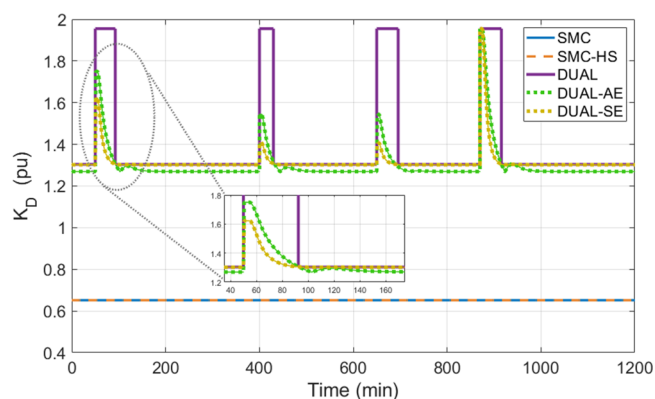
Figure 13. Evolution over time of K_D for the tracking performance test.

dual-mode SMCs. The dual controller gains switch between fixed values when the change between High and Low gain occurs, giving more abrupt controller outputs than the other dual-mode schemes, as shown in Figure 12. Moreover, nonlinear K_D gains (DUAL-AE and DUAL-SE) evolution shows that in the "transient region", the gain is increased

accordingly with the amplitude of the set point change when the error is significant. It decreases as the error goes to the "around steady-state region", where the controller gains its "Low Gain" value. The DUAL-AE gain has a greater amplitude in the transient than the DUAL-SE gain, requiring more time to compensate for the error.

In summary, Figure 13 shows the importance of the H and L parameters to the performance of the proposed controllers in the "transient region" and the "around the steady-state region", respectively.

Moreover, a radial graph to compare the indices and transient criteria for this process is presented in Figure 14. The chart compares the maximum overshoot, ITSE, and TVu. The Mp is considered for the set point changes at minute 50 for Mp1 and 870 for Mp2.
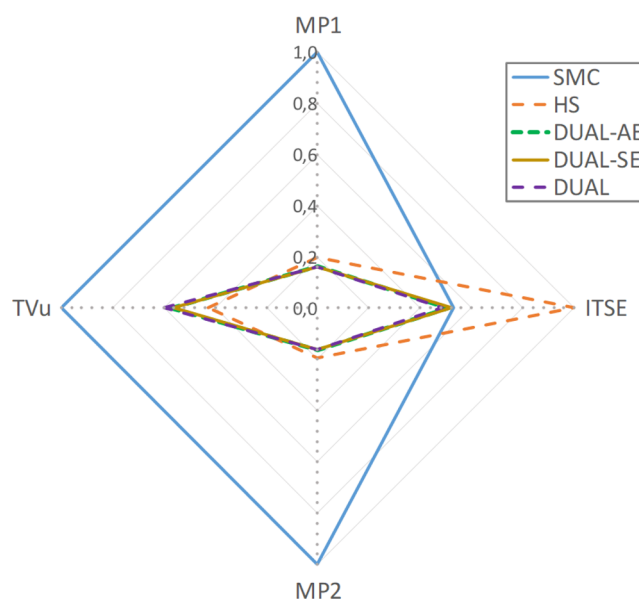
Figure 14. Radial graph for tracking.

The radial graph shows that dual-mode schemes have a very close area, almost the same for the three schemes. The dual-mode schemes present an 80% reduction compared to the SMC in maximum overshoot. ITSE decreased by 50% compared to HS, indicating the improvement in the transient response of the proposal approach improvement by ref 27. Finally, in TVu, the control law performance is improved by 40%, close to its predecessor SMC-HS value, which shows an improvement of 50%. All dual schemes have better characteristics than previous SMCs.

4.2. Mixing Tank. The second example considers a mixing tank, as is shown in Figure 15. This example is important for industrial process engineering. Food and beverage manufacturing requires product mixing. This process mixes raw materials in precise proportions and controls environmental elements like temperature.[56,57]

The tank receives two streams, a hot stream, $W_1(t)$, and a cold stream, $W_2(t)$. The outlet temperature is measured at 125 ft downstream from the tank. The following assumptions are accepted:

- The liquid volume in the tank is considered constant.
- The tank contents are well mixed.
- The tank and the pipe are well insulated.
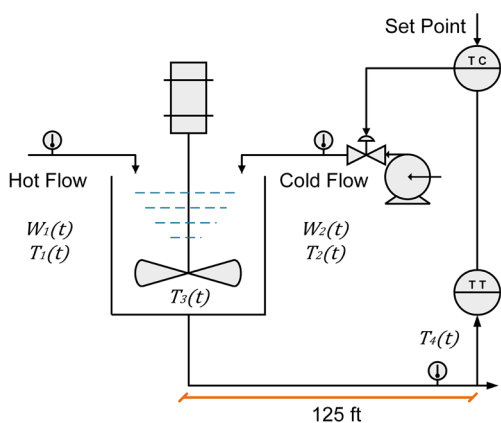
Figure 15. Mixing tank process diagram.

The mixing tank nonlinear equations and operating conditions are presented in.[4] However, it is remarkable to present the mathematical relationships between the temperature $T_3(t)$ inside the Tank and $T_4(t)$ measured after the time delay. The delay is modeled as a function of the characteristics of the length L and area A of the connecting pipe as well as the density ρ of the fluid. The expression of the delay in this plant is given by eq 51:

$$t_0 = \frac{LA\rho}{W_1(t) + W_2(t)} \tag{51}$$

Thus, the relationship between $T_3(t)$ and $T_4(t)$ can be simply described as eq 52 presents:

$$T_4(t) = T_3(t - t_0) \tag{52}$$

The control objective in this process is to keep the temperature constant inside the tank. The transmitter manages a range from 100−200 °F, and the valve handles values from 0 to 1 per unit value (pu). At initial conditions, the temperature of the liquid in the mixing tank is 150 °F. Again, the nonlinear process model is approximated to a FOPDT model following a similar procedure as the reactor. Therefore, the reaction curve method described by ref 13 was used. The FOPDT model representing its dynamics is shown in eq 53:

$$G_{p_1}(s) = \frac{-0.8754}{2.4749s + 1}e^{-4.3749s} \tag{53}$$

The controllability ratio (t_0/τ) is associated with the difficulty level in controlling a process.[58] It is also known as the normalized dead time or the normalized time delay.[59] Generally speaking, processes with small (t_0/τ) are simple to regulate, and as a system gets bigger (t_0/τ), it is harder to control. Generally, it may say that processes with a small value of this parameter can be easily controlled, whereas processes with a greater value can be deemed more difficult to control. In this example, (t_0/τ) is greater than one, which is a difficult process to control, which represents a process with a dominant time delay.

Additionally, this delay is variable accordingly with any mass flow variation. Finally, it is remarked that the actual condition of the tank is considered in a constant level because the liquid volume is considered also constant as indicated in the previous assumptions.

Similar to the CSTR case, once the values of K, τ, and t_0 are known, the values of λ_0, λ_1, δ, and K_{DO} can be calculated using eqs 34−37. Meanwhile, the design parameter values for the

dual schemes H, L, e_{max}, and e_{min} were chosen equal to those of the CSTR case ($H = 3$, $L = 2$, $e_{max} = 0.5$, and $e_{min} = 0.025$). Table 2 details all the remaining parameter values that the controllers take for this process.

Table 2. Controllers Parameter Values

parameter	controller				
	SMC	SMC-HS	DUAL	DUAL-AE	DUAL-SE
K_{D0}	0.4534				
λ_0	0.1				
λ_1	0.6326				
δ	0.7101				
γ				2.1053	
ρ				1.9474	
ϕ					4.01
θ					1.9975
$K_D\|_{e(t)=0}$	K_{D0}	K_{D0}	0.9069	0.883	0.9057

4.2.1. Regulation Performance Test. Disturbances in the flow of hot water are added, and changes are introduced from 250 lb/min to 150 lb/min, reducing 25 lb/min four times. Those changes can be seen in Figure 16.
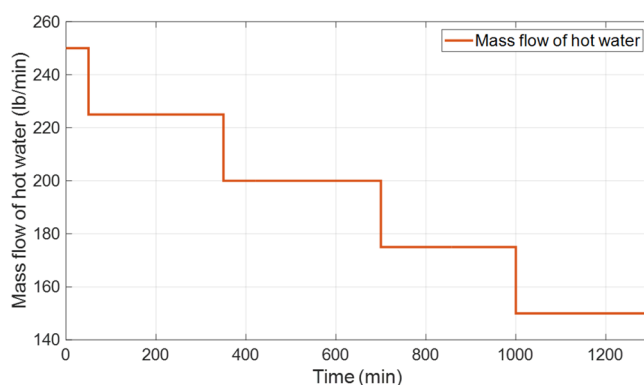
Figure 16. Variation of hot water mass flow.

As mentioned above, this process has a dominant delay that additionally is variable. For example, Figure 17 shows the delay variation when the hot water flow disturbances appear; an increment in the time delay performs until a transportation lag close to 6 min.
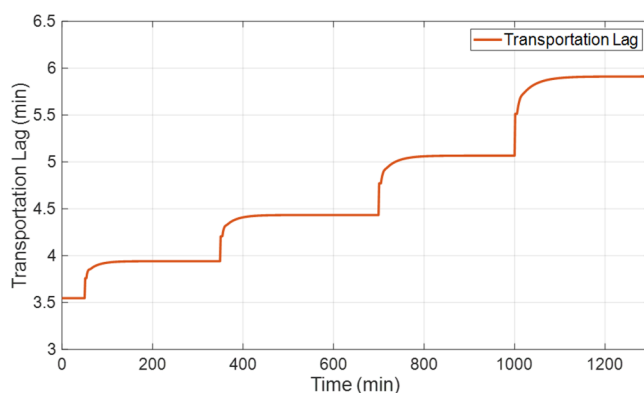
Figure 17. Delay variation due to disturbances in the system.

This increase in the variable delay will be reflected as a difference between the liquid temperature in the mixing tank $T_3(t)$ and temperature $T_4(t)$, which is the one from which the measurement will be obtained after the delay. Figure 18 shows
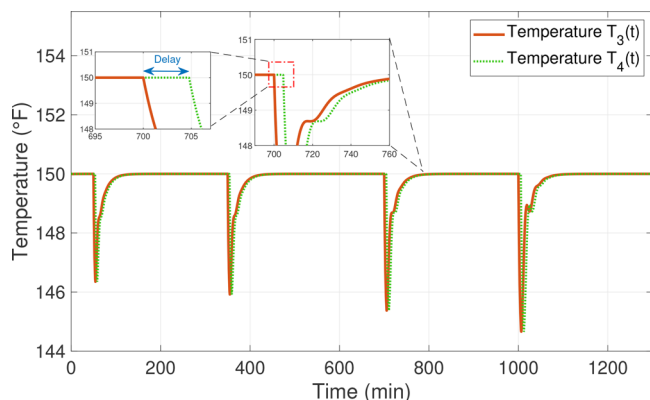
Figure 18. System outputs comparison regarding the variable delay.

the temperature output controlled with a SMC-DUAL scheme. Both $T_3(t)$ and $T_4(t)$ are presented, which in long operation times practically seem to be the same output. However, if an approximation is made such as those shown on the left side of Figure 18, it can be seen that there is a phase shift between the signals due to the variable delay. As can be seen in Figure 17, the delay for the operation time of around 700 min corresponds approximately to five additional minutes. As system disturbances increase, this delay also increases.

Figure 19 shows how all the SMC approaches compensate for the disturbances. Similar to the CSTR case, the responses
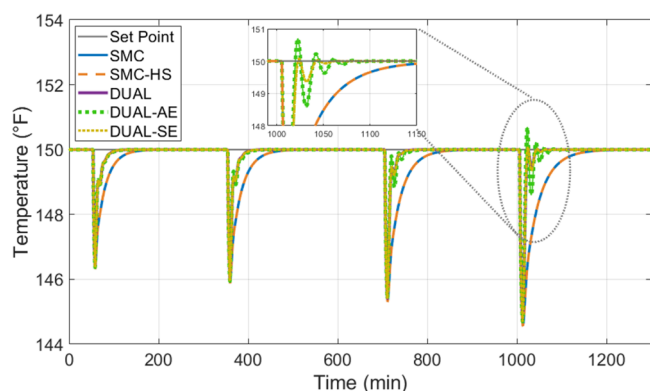
Figure 19. System outputs when hot water mass flow disturbances are introduced.

of the process for the SMC and SMC-HS controllers are equal; they have slower disturbance rejection responses and are overlapped since they have the same constant gain, K_{DO}. Meanwhile, the dual-mode SMC schemes reject the disturbances more quickly. Although their process responses are similar most of the time, the DUAL-AE controller process output presents an overshoot and some oscillations when the more considerable transportation lag is achieved (starting at a time equal to 1000 min). So, the time delay affects most of the DUAL-AE controller system response.

Figure 20 shows all the SMC controller outputs, and their responses follow the observed temperature response. The traditional SMC and the SMC-HS controller scheme outputs
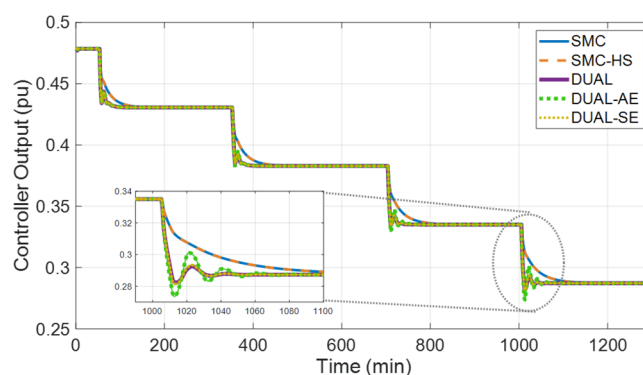
Figure 20. Control outputs when disturbances occur.

present smooth variations for the actuator, but they reject the disturbances slower than the dual-mode controller schemes. So, the dual-mode controller schemes are more aggressive; faster responses also require faster control actions; however, these variations are not abrupt enough to deteriorate the final control element. Only the DUAL-AE controller output presents a slight overshoot and oscillations. Still, just in the worst case, when the most considerable time delay is present, the most significant modeling error is acting. However, the controller performance is good enough, rejecting the actual disturbance.

Figure 21 shows K_D evolution for the different controllers. As in the CSTR case, it is evident that the SMC and SMC-HS
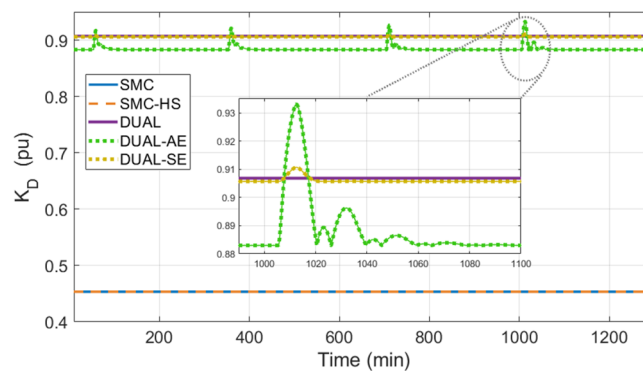
Figure 21. Evolution over time of K_D for regulation performance tests.

controller gains are smaller than those for the dual-mode SMCs, giving a sluggish system performance. There is no switching between the "around steady-state region" and the "transient region" because no set point change occurs during the test since only regulation tasks are performed. When the disturbances arise, the system remains on the "around the steady-state region" when the output error $e(t)$ grows in magnitude; only the DUAL-AE increases smoothly to correct the error. Again, at steady-state, the DUAL and DUAL-SE gains are close to each other and slightly higher than the DUAL-AE gain, giving the desired aggressiveness established by the design parameter L for the "around the steady-state region".

Finally, the performance of the controllers is compared quantitatively on a radial graph in Figure 22. As in the process mentioned above, the dual schemes have the smallest area. In this process, using an SMC or SMC-HS offers the same results since only regulation tests are performed, and they use the K_{DO} gain. Therefore, enhancements come with dual controllers.
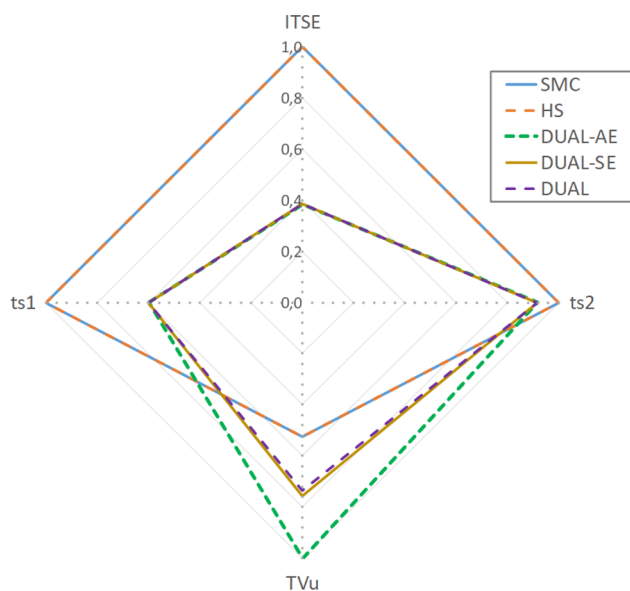
Figure 22. Radial graph for dead time variations.

The t_{s1} is improved by 40%, and the ITSE was enhanced by up to 60%. The controller that obtains the smallest area on the radial graph is the DUAL and the DUAL-SE. For this system, using the dual variation that considers the squared error would be convenient. However, the DUAL controller is not recommended because it does not consider smooth switching.

The mixing tank dynamics are abrupt, requiring a controller that quickly compensates it, as DUAL-SE does. According to the process requirement, changing the H/L ratio can help obtain less aggressive responses; this could be improved by decreasing the H value.

5. CONCLUSIONS

This paper has shown dual-mode sliding mode controller synthesis based on a FOPDT model of the actual process. The proposed approach enhanced tracking and regulation by following the dual mode concepts. The new control structure changes between PD and PID sliding surfaces. The PD surface improves the tracking transient response against set point changes, avoiding overshoot and oscillations and switching to the PID surface when the system output is close to the set point to guarantee zero steady-state error. Four desired control objectives were established to obtain a well-defined control problem design.

Three different reaching gains were proposed for the dual-mode control schemes to get an appropriate (High Gain)/(Low Gain) relationship. In addition, a smooth switching transition between PD/PID SMC controllers ensured closed-loop stability when the proposed nonlinear gains were used.

The computer simulation examples indicated that the proposed dual-mode SMC controller performance is stable and satisfactory despite nonlinearities over various operating conditions, set point changes, process disturbances, and modeling errors. Furthermore, it showed the dual-mode scheme improvement for tracking and regulatory tasks. Thus, the new H and L design parameter influence to obtain the above improvements in the "transient region" and the "around the steady-state region," respectively, was noticed. Remarkably, the dual schemes with nonlinear gain balance the speed of response and the control action smoothness. Thus, quick

control was attained, considering the incidence over the final control elements.

A comparative evaluation to determine the proposal performance is done in two nonlinear processes, one with variable delay. The merits and drawbacks of each modified scheme were analyzed using radial graphs, comparing the control methods with different performance measures for set point and disturbance changes.

Summarizing, the main novelties and contributions are the design and implementation of a controller combining dual-mode control concepts and sliding mode control methodology; the controller synthesis is based on the approximation of FOPDT to avoid the design from a complex model. A new controller uses the combination of higher gain to large error signals (transient) and lower gain to small error signals (the region around the set point).

■ AUTHOR INFORMATION

Corresponding Author

Oscar Camacho − *Colegio de Ciencias e Ingenierias, Universidad San Francisco de Quito USFQ, Quito 170157, Ecuador;* ◉ orcid.org/0000-0001-8827-5938; Email: ocamacho@usfq.edu.ec

Authors

Camila Obando − *Dipartimento di Informatica, Modellistica, Elettronica e Sistemistica, Università della Calabria, 87036 Rende, Italy*

Ruben Rojas − *Escuela de Ingeniería Eléctrica, Facultad de Ingeniería, Universidad de Los Andes, Mérida 5101, Venezuela*

Francisco Ulloa − *Dipartimento di Informatica, Modellistica, Elettronica e Sistemistica, Università della Calabria, 87036 Rende, Italy*

Complete contact information is available at:
https://pubs.acs.org/10.1021/acsomega.2c08201

Author Contributions

O.C., conception of the idea, preparation of the first draft, and final manuscript review. C.O., methodology, preparation of the first draft, simulations and graphs besides designing, and reviewed the final manuscript. R.R., designed the initial draft and reviewed the final manuscript. F.U., reviewed and helped with the final manuscript.

Notes

The authors declare no competing financial interest.

■ REFERENCES

(1) Lee, J. H.; Lee, J. M. Progress and challenges in control of chemical processes. *Annu. Rev. Chem. Biomol. Eng.* **2014**, *5*, 383−404.

(2) Nandakumar, K.; Joshi, J. B.; Valsaraj, K. T.; Nigam, K. D. Perspectives on Manufacturing Innovation in Chemical Process Industries. *ACS Engineering Au* **2022**, *2*, 3−11.

(3) Sardella, M. F.; Serrano, E.; Camacho, O.; Scaglia, G. Linear Algebra Controller Design Based on the Integral of Desired Closed-Loop Behavior: Application to Regulation and Trajectory Tracking in a Typical Chemical Process. *Ind. Eng. Chem. Res.* **2020**, *59*, 20131−20140.

(4) Camacho, O.; Smith, C. A. Sliding mode control: an approach to regulate nonlinear chemical processes. *ISA Transactions* **2000**, *39*, 205−218.

(5) Utkin, V.; Poznyak, A.; Orlov, Y. V.; Polyakov, A. *Road map for sliding mode control design*; Springer, 2020.

(6) Khalil, H. K. *Nonlinear control*; Pearson: New York, 2015; Vol. *406*.

(7) Mehta, A.; Bandyopadhyay, B. *Emerging Trends in Sliding Mode Control: Theory and Application*; Springer, 2021.

(8) Kadu, C.; Khandekar, A.; Patil, C. Design of sliding mode controller with proportional integral sliding surface for robust regulation and tracking of process control systems. *Journal of Dynamic Systems, Measurement, and Control* **2018**, *140*, 091004.

(9) Wang, H.; Wang, Z.; Zhou, Q.; Liang, J.; Yin, Y.; Su, W.; Wang, G. Optimization and sliding mode control of dividing-wall column. *Ind. Eng. Chem. Res.* **2020**, *59*, 20102−20111.

(10) Cargua-Sagbay, D.; Palomo-Lema, E.; Camacho, O.; Alvarez, H. Flash Distillation Control Using a Feasible Operating Region: A Sliding Mode Control Approach. *Ind. Eng. Chem. Res.* **2020**, *59*, 2013−2024.

(11) Prado, A. J.; Herrera, M.; Dominguez, X.; Torres, J.; Camacho, O. Integral Windup Resetting Enhancement for Sliding Mode Control of Chemical Processes with Longtime Delay. *Electronics* **2022**, *11*, 4220.

(12) Ogunnaike, B. A.; Ray, W. H. *Process dynamics, modeling, and control*; Oxford University Press, 1994.

(13) Smith, C. A.; Corripio, A. B. *Principles and practices of automatic process control*; John Wiley & Sons, 2005.

(14) Muresan, C. I.; Ionescu, C. M. Generalization of the FOPDT model for identification and control purposes. *Processes* **2020**, *8*, 682.

(15) Sardella, M. F.; Serrano, M. E.; Camacho, O.; Scaglia, G. J. Design and application of a linear algebra based controller from a reduced-order model for regulation and tracking of chemical processes under uncertainties. *Ind. Eng. Chem. Res.* **2019**, *58*, 15222−15231.

(16) Camacho, O.; Smith, C.; Moreno, W. Development of an Internal Model Sliding Mode Controller. *Ind. Eng. Chem. Res.* **2003**, *42*, 568−573.

(17) Salinas, L. R.; Santiago, D.; Slawiñski, E.; Mut, V. A.; Chavez, D.; Leica, P.; Camacho, O. P+ d plus sliding mode control for bilateral teleoperation of a mobile robot. *International Journal of Control, Automation and Systems* **2018**, *16*, 1927−1937.

(18) Báez, E.; Bravo, Y.; Leica, P.; Chávez, D.; Camacho, O. Dynamical sliding mode control for nonlinear systems with variable delay. *2017 IEEE 3rd Colombian Conference on Automatic Control (CCAC)*; IEEE, 2017; pp 1−6.

(19) Proaño, P.; Capito, L.; Rosales, A.; Camacho, O. Sliding Mode Control: Implementation Like PID for Trajectory-Tracking for Mobile Robots. *2015 Asia-Pacific Conference on Computer Aided System Engineering*; IEEE, 2015; pp 220−225.

(20) Espín, J.; Castrillon, F.; Leiva, H.; Camacho, O. A modified Smith predictor based−Sliding mode control approach for integrating processes with dead time. *Alexandria Engineering Journal* **2022**, *61*, 10119−10137.

(21) Herrera, M.; Camacho, O.; Leiva, H.; Smith, C. An approach of dynamic sliding mode control for chemical processes. *Journal of Process Control* **2020**, *85*, 112−120.

(22) Morales, L.; Estrada, J. S.; Herrera, M.; Rosales, A.; Leica, P.; Gamboa, S.; Camacho, O. Hybrid Approaches-Based Sliding-Mode Control for pH Process Control. *ACS Omega* **2022**, *7*, 45301−45313.

(23) Camacho, O.; Rojas, R.; García-Gabín, W. Some long time delay sliding mode control approaches. *ISA Transactions* **2007**, *46*, 95−101.

(24) Iglesias, E.; García, Y.; Sanjuan, M.; Camacho, O.; Smith, C. Fuzzy surface-based sliding mode control. *ISA Transactions* **2007**, *46*, 73−83.

(25) Bandyopadhyay, B.; Abera, A. G.; Janardhanan, S.; Sreeram, V.; et al. Sliding mode control design via reduced order model approach. *International Journal of automation and Computing* **2007**, *4*, 329−334.

(26) Proaño, P.; Capito, L.; Rosales, A.; Camacho, O. A dynamical sliding mode control approach for long deadtime systems. *2017 4th International Conference on Control, Decision and Information Technologies (CoDIT)*; IEEE, 2017; pp 0108−0113.

(27) Rojas, R.; Camacho, O.; González, L. A sliding mode control proposal for open-loop unstable processes. *ISA Transactions* **2004**, *43*, 243−255.

(28) Camacho, O.; De la Cruz, F. Smith predictor based-sliding mode controller for integrating processes with elevated deadtime. *ISA Transactions* **2004**, *43*, 257−270.

(29) Pérez de la Parte, M.; Camacho, O.; Camacho, E. F. Development of a GPC-based sliding mode controller. *ISA transactions* **2002**, *41*, 19−30.

(30) Espín, J.; Estrada, S.; Benítez, D.; Camacho, O. A hybrid sliding mode controller approach for level control in the nuclear power plant steam generators. *Alexandria Engineering Journal* **2023**, *64*, 627−644.

(31) Castellanos-Cárdenas, D.; Castrillón, F.; Vásquez, R. E.; Posada, N. L.; Camacho, O. A new Sliding Mode Control tuning approach for second-order inverse-response plus variable dead time processes. *Journal of Process Control* **2022**, *115*, 77−88.

(32) Obando, C.; Chávez, D.; Leica, P.; Camacho, O. Sliding Mode Controller Based on a Hybrid Surface for Tracking Improvement of Non-Linear Processes. *IFAC-PapersOnLine* **2020**, *53*, 11747−11752.

(33) Liu, J.; Wang, X. *Advanced sliding mode control for mechanical systems*; Springer, 2012.

(34) Slotine, J.-J. E.; Li, W. *Applied nonlinear control*; Prentice Hall: Englewood Cliffs, NJ, 1991; Vol. *199*.

(35) Feldbaum, A. A. Dual control theory. I. *Avtomat. i Telemekh.* **1960**, *21*, 1240−1249.

(36) Feldbaum, A. A. Dual control theory. II. *Avtomat. i Telemekh.* **1960**, *21*, 1453−1464.

(37) Feldbaum, A. A. Theory of dual contro. *Avtomat. i Telemekh.* **1961**, *22*, 3−16.

(38) Feldbaum, A. A. Dual control theory. IV. *Avtomat. i Telemekh.* **1961**, *22*, 129−142.

(39) Shinskey, F.; Weinstein, J. A dual-mode control system for a batch exothermic reactor. *Twentieth Annual ISA Conference, Los Angeles*; ISA, 1965.

(40) Shinskey, F. G. *Process control systems*; McGraw-Hill, Inc., 1979.

(41) De Santis, R. M. A Novel PID Configuration for Speed and Control. *Journal of Dynamic Systems Measurement and Control, ASME Trans* **1994**, *116*, 351−323.

(42) Wittenmark, B. Adaptive Dual Control Methods: An Overview. *5th IFAC Symposium on Adaptive Systems in Control and Signal Processing 1995*; IFAC: Budapest, Hungary, June 14−16, 1995; Vol. 28, pp 67−72.

(43) Allgöwer, F.; Ogunnaike, B. Dual-mode adaptive control of nonlinear processes. *Comput. Chem. Eng.* **1997**, *21*, S155−S160. Supplement to Computers and Chemical Engineering

(44) Unbehauen, H. Adaptive dual control systems: A survey. *Proceedings of the IEEE 2000 Adaptive Systems for Signal Processing, Communications, and Control Symposium (Cat. No.00EX373)*; IEEE, 2000; pp 171−180.

(45) Viswanathan, K.; Oruganti, R.; Srinivasan, D. Dual-mode control of tri-state boost converter for improved performance. *IEEE Transactions on Power Electronics* **2005**, *20*, 790−797.

(46) Cho, W.; Edgar, T. F.; Lee, J. Iterative learning dual-mode control of exothermic batch reactors. *Control Engineering Practice* **2008**, *16*, 1244−1249.

(47) Bhattarai, R.; Gurung, N.; Kamalasadan, S. Dual Mode Control of a Three-Phase Inverter Using Minimum Variance Adaptive Architecture. *IEEE Transactions on Industry Applications* **2018**, *54*, 3868−3880.

(48) Diaz, C. J. L.; Ocampo-Martinez, C.; Olaru, S. Dual mode control strategy for the energy efficiency of complex and flexible manufacturing systems. *Journal of Manufacturing Systems* **2020**, *56*, 104−116.

(49) Fang, H.; Chen, L.; Shen, Z. *Comparison of Different Integral Performance Criteria for Optimal Hydro Generator Governor Tuning*

with a Particle Swarm Optimization Algorithm; Computational Science − ICCS 2007: Berlin, Heidelberg, 2007; pp 1186−1189.

(50) Edwards, C.; Spurgeon, S. *Sliding mode control: theory and applications*; CRC Press, 1998.

(51) DeCarlo, R.; Zak, S.; Matthews, G. Variable structure control of nonlinear multivariable systems: a tutorial. *Proceedings of the IEEE* **1988**, *76*, 212−232.

(52) Beker, O.; Hollot, C.; Chait, Y.; Han, H. Fundamental properties of reset control systems. *Automatica* **2004**, *40*, 905−915.

(53) de Haan, A. B.; Padding, J. T. *Process Technology*; De Gruyter, 2022.

(54) Luyben, W. L. *Chemical reactor design and control*; John Wiley & Sons, 2007.

(55) Edeleva, M.; Marien, Y. W.; Van Steenberge, P. H.; D'hooge, D. R. Jacket temperature regulation allowing well-defined non-adiabatic lab-scale solution free radical polymerization of acrylates. *Reaction Chemistry & Engineering* **2021**, *6*, 1053−1069.

(56) Halász, L. *Control methods in polymer processing*; Elsevier, 2012.

(57) Akbariza, M.; Handoko, D.; Prajitno, P. Temperature and water level control in a multi-input, multi-output process using neuro-fuzzy controller. *Journal of Physics: Conference Series* **2021**, *1816*, 012022.

(58) Gude, J. J.; García Bringas, P. Proposal of a General Identification Method for Fractional-Order Processes Based on the Process Reaction Curve. *Fractal and Fractional* **2022**, *6*, 526.

(59) Åström, K. J.; Hägglund, T.; Astrom, K. J. *Advanced PID control*; ISA-The Instrumentation, Systems, and Automation Society Research Triangle Park, 2006; Vol. *461*.